Journal of Ceramic Processing Research. Vol. 15, No. 6, pp. 535~538 (2014)

JOURNAL OF
Ceramic
Processing Research

Effect of an oxide buffer layer on the power conversion efficiency in inverted P3HT : PCBM organic photovoltaic cells

Rajagembu Perumal, Narayanasamy Sabari Arul and Tae Whan Kim*
Department of Electronics and Computer Engineering, Hanyang University, 222 Wangsimni-ro, Seongdong-gu, Seoul 133-791, Korea

The influence of the oxide buffer layer (OBL) on the power conversion efficiency (PCE) in inverted poly (3-hexylthiophene) : fullerene derivative [6,6]-phenyl-C61-butyric acid methyl ester (P3HT : PCBM) photovoltaic cells was investigated. Three different hole buffer layers (HBLs) of poly (3,4-ethylenedioxythiophene): poly (styrene sulfonate) (PEDOT : PSS), tungsten-oxide (WO_3), or molybdenum-oxide (MoO_3) were used to improve the charge generation between the P3HT : PCBM and the Ag electrode. Atomic force microscopy images showed that the surface of the P3HT:PCBM active layer with a MoO_3 OBL was smoother that with a PEDOT : PSS layer or a WO_3 layer and without a HBL. The PCE of the OPV cells with a MoO_3 OBL was higher than those of the inverted OPV cells with a PEDOT : PSS layer or a WO_3 layer and without a HBL. The inverted OPV cells containing a MoO_3 OBL with a high-work function provided a large interface between the P3HT : PCBM active layer and the Ag electrode due to charge generation, resulting in an enhancement of the device performances for the OPV cells with a MoO_3 OBL.

PACS numbers: 72.40.+w, 82.47.Jk, 78.30.Jw
Key words: Organic photovoltaic cells, Oxide buffer layer, Power conversion efficiency, Inverted structure.

Introduction

Harvesting energy directly from the sunlight using photovoltaic technology has been extensively recognized as a crucial component of future global energy production [1]. Organic photovoltaic (OPV) cells, which directly convert sunlight into electricity, have been receiving considerable attention due to their high-mechanical flexibility, low cost, and simple fabrication process [2-4]. The prospect of promising applications of OPV cells in optoelectronic devices has led to substantial research and development efforts to enhance the power conversion efficiency (PCE) and the life time of the OPV cells [5]. Poly(3,4-ethylenedioxythiophene) : poly(styrene sulfonate) (PEDOT : PSS) is commonly used as a hole transport layer of the PEDOT : PSS in OPV devices to facilitate extraction of photogenerated holes, and to ensure that electrons flow into the cathode. Unfortunately, the stability and life time of the OPV devices was affected due to the acidic nature, hygroscopic and low stability of PEDOT : PSS layer [6-8]. A frequently employed structure to solve this issue is to invert the layer structure.

OPV cells with an inverted device architecture, in which the positions of the anode and cathode were reversed, were employed in order to overcome these problems [9, 10]. The efficiency of the fabricated inverted OPV cells is significantly affected by a hole buffer layer (HBL), such as a PEDOT : PSS layer, a tungsten-oxide (WO_3) layer, or a molybdenum-oxide (MoO_3) layer [11, 12]. Among the various kinds of the HBLs, the PEDOT : PSS layer deteriorates the device performance of the OPV cells due to a chemical reaction with the electrodes and to damage to the active layer [13]. The HBL with a low-work function was susceptible to the degradation of the OPV cells due to the existence of the oxygen and moisture, resulting in the deterioration of the device performance [14]. A transparent metal-oxide HBL with a high-work function, which affects effective hole injection efficiency and high-chemical stability, can encounter major problems of PEDOT : PSS layer [15, 16]. Even though some investigations concerning the device characteristics of inverted OPV cells containing a PEDOT : PSS HBL have performed to enhance their PCEs and lifetimes, very few studies on the fabrication of inverted OPV cells with alternative HBLs instead of the PEDOT : PSS HBL have been performed.

This paper reports data for the effect of an oxide buffer layer (OBL) on the PCE in inverted P3HT : PCBM OPV cells. Atomic force microscopy (AFM) measurements were performed to determine the surface morphologies of the poly (3-hexylthiophen) : [6,6]-phenyl-C61-buytyric acid methyl ester (P3HT : PCBM) active layer with and without a HBL layer. Current density-voltage (J-V) measurements were performed to investigate the electrical characteristics of the fabricated OPV cells with various HBLs.

*Corresponding author:
Tel : +82-2-2220-0354
Fax: +82-2-2292-4135
E-mail: twk@hanyang.ac.kr

Experimental Details

The inverted OPV cells with a HBL fabricated in this study were prepared on indium-tin-oxide (ITO)-coated glass substrates, and the sheet resistance of the ITO thin film was approximately 10 Ω/sq. The ITO substrates were cleaned in acetone and isopropanol for 10 min by using an ultrasonic cleaner and were rinsed in de-ionized water thoroughly. After the chemically cleaned ITO substrates had been dried by using N_2 gas with a purity of 99.99%, the surfaces of the ITO substrates were treated with an ultraviolet-ozone cleaner for 10 min at room temperature. After the prepared ITO substrates had been introduced into a glove box with a high-purity N_2 atmosphere, the ZnO solution was coated on the ITO substrates by using spin coating at 3000 rpm for 31 s [17, 18]. The active layer was prepared by dissolving P3HT:PCBM in a molar ratio of 1 : 0.8 using 1-2 dichlorobenzene as solvent [19]. The mixed solution was stirred for 15 h under continuous stirring at 50°C. Then, the solution was deposited on the PEDOT : PSS layer by using spin coating at 1500 rpm for 61s and was annealed at 145°C for 10 min. A WO_3 or MoO_3 OBL with thickness of 10 nm was deposited by using thermal evaporation. Then, an Ag layer with a thickness of 80 nm was formed by using thermal evaporation. Schematic diagrams of the structures and the energy levels of the fabricated Ag/HBLs/P3HT : PCBM/ZnO/ITO cells with various HBLs are shown in Fig. 1.

AFM measurements were carried out to investigate the surface properties of the P3HT : PCBM active layer with and without a HBLs. J-V measurements were performed to investigate the photovoltaic characteristics of the inverted OPV cells with various HBLs under AM 1.5 simulated illumination with an intensity of 100 mW/cm^2.

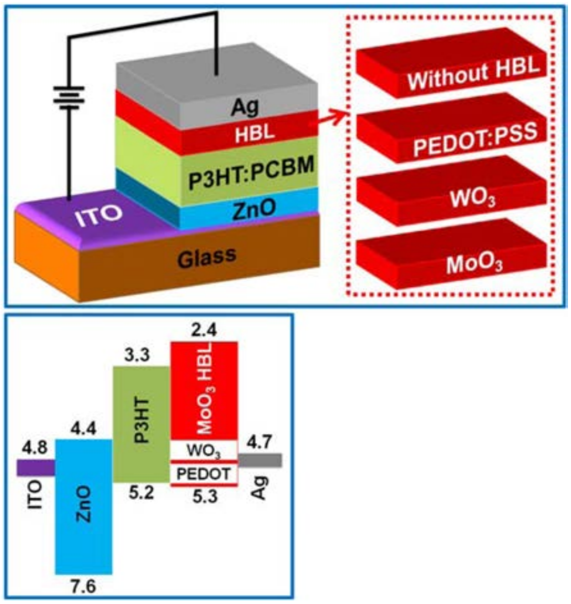

Fig. 1. Schematic diagrams of the device structures and the corresponding energy band diagrams of the inverted OPV cell with a HBL.

Result and Discussions

Figure 2 shows the AFM profile images of the P3HT:PCBM photoactive layer (a) without a HBL, (b) with a PEDOT : PSS HBL, (c) with a WO_3 OBL, and (d) with a MoO_3 OBL. The average root-mean-square roughness value of the P3HT:PCBM photoactive layers without a HBL and with a PEDOT : PSS HBL, a WO_3 OBL, or a MoO_3 OBL are 0.935, 2.042, 2.13, and

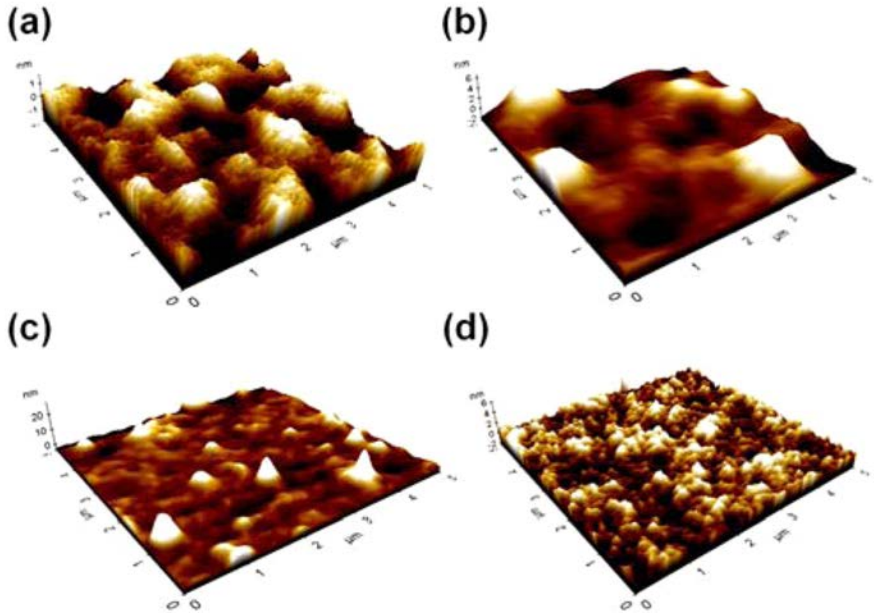

Fig. 2. AFM profile images of the P3HT : PCBM (a) without HBL, (b) PEDOT : PSS HBL, (c) WO_3 OBL, and (d) MoO_3 OBL.

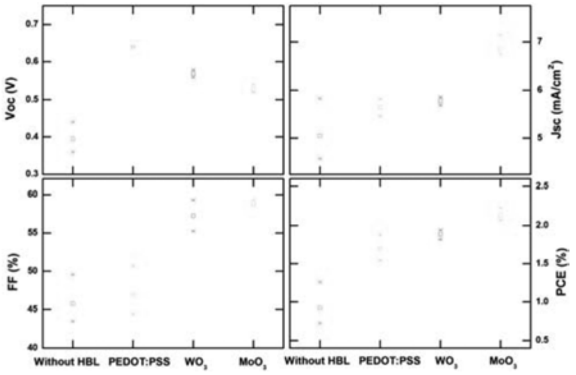

Fig. 3. Statistical box graphs for the J_{sc}, the V_{oc}, the FF, and the PCE for 28 devices.

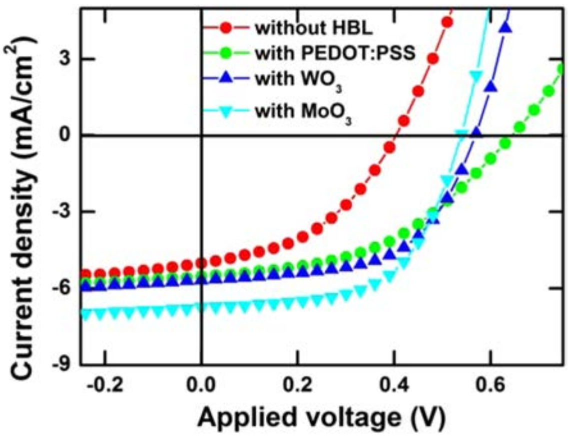

Fig. 4. J-V results for inverted OPV cells utilizing with and without HBLs under 100 mW/cm^2.

0.669 nm, respectively. AFM profile images showed that the P3HT : PCBM active layer with a MoO_3 OBL had the best smoothness and the lowest pinhole density with a low surface roughness. The surface of the P3HT : PCBM active layer with a MoO_3 OBL showed the best morphology among those of the P3HT : PCBM active layers with HBLs.

Figure 3 shows the statistical box chart for 28 numbers of the fabricated OPV cells. The statistical box charts showed that V_{oc} and J_{sc} values of the inverted OPV cells without a HBL are unstable and lower than those of the inverted OPV cells with a HBL. However, the V_{oc} and J_{sc} of the inverted OPV cell with a HBL are significantly improved due to the high-work function of the inserted HBL [20].

Even though the electrical characteristics measurement was performed for several inverted OPV cells, only the results for the best performance of the inverted OPV cells were described in Fig. 4. Fig. 4 shows the J-V curves of the fabricated inverted OPV cells utilizing various HBLs. The device performances of the inverted OPV cells utilizing various HBLs are summarized in Table 1. The PCE, FF, J_{sc}, and V_{oc} of the inverted OPV

Table 1. Device performance of inverted OPV cells utilizing various HBLs.

HBL	V_{oc} (V)	J_{sc} (mA/cm^2)	FF (%)	PCE (%)
Without	0.40	5.01	43.51	0.88
PEDOT : PSS	0.64	5.53	45.39	1.62
WO_3	0.57	5.69	56.96	1.85
MoO_3	0.54	6.74	58.58	2.14

cells without a HBL are 0.88%, 43.51, 5.01 mA/cm^2, and 0.40 V, respectively. The leakage current of the inverted OPV cells without a HBL increases at the contact between the cathode electrode and the active layer due to the better morphology and the smaller hole collection.

OPV cells performances were significantly improved after inserting HBLs. The PCE, J_{sc}, and FF of the inverted OPV cells with a WO_3 OBL are 1.85%, 5.69 mA/cm^2, and 56.96, respectively. The PCE, J_{sc}, and FF of the inverted OPV cells with a MoO_3 OBL are 2.14%, 6.74 mA/cm^2, and 58.58, respectively. The PCE of the inverted OPV cell with a MoO_3 OBL is higher than that of the inverted OPV cell with a PEDOT : PSS or WO_3 HBL due to a lowest pinhole density with low surface roughness provides a large interface between the P3HT : PCBM active layer and the Ag electrode. The LUMO levels of WO_3 or MoO_3 layer can provide a significant energy barrier for electrons in PCBM and meanwhile the chance of electron recombination were suppressed near the anodes [21]. The LUMO level of MoO_3 is higher than that of general donor materials [22], the of MoO_3 OBL can act as an effective electron blocking layer compared with the inadequate capability of PEDOT : PSS [23]. Furthermore, MoO_3 is regarded as a very stable material which can serve as a protective layer to prevent undesired physical and chemical reactions between Ag and P3HT:PCBM active layers [24], resulting in an enhancement of the device performances for the OPV cells with a MoO_3 OBL.

Conclusions

Inverted OPV cells with a PEDOT : PSS, a WO_3, or a MoO_3 HBLs were fabricated to investigate their improvement in the PCEs. AFM images showed that the surface of the P3HT : PCBM active layer with a MoO_3 OBL was smoother that with a PEDOT : PSS layer or a WO_3 layer and without a HBL. The PCE of the OPV cells with a MoO_3 OBL was 2.14% higher than that of the inverted OPV cells without a HBL. The inverted OPV cells containing a MoO_3 OBL with a high-work function provided a large interface between the P3HT:PCBM active layer and the Ag electrode due to charge generation, resulting in an enhancement of the device performances for the OPV cells with a MoO_3 OBL.

Acknowledgments

This research was supported by Basic Science Research Program through the National Research Foundation of Korea (NRF) funded by the Ministry of Education, Science and Technology (2013-016467).

References

1. P. W. M. Blom, V. D. Mihailetchi, L. J. A. Koster, and D. E. Markov, Adv. Mater. 19 (2007) 1551-1566.
2. Y. Kim, S. A. Choulis, J. Nelson, D. D. D. Bradley, S. Cook, and J. R. Durrant, Appl. Phys. Lett. 86 (2005) 063502-1-063502-3.
3. J. Peet J, J. Y. Kim, N. E. Coates, M. L. Ma, D. Moses, A. J. Heeger, and G. C. Baza, Nat. Mater. 6 (2007) 497-500.
4. G. Dennler, M. C. Scharber, and C. J. Brabec, Adv. Mater. 21 (2009) 1323-1338.
5. L. M. Chen, Z. Hong, G. Li, and Y. Yang, Adv. Mater. 21 (2009) 1434-1449.
6. X. H. Yang, F. Jaiser, B. Stiller, D. Neher, F. Galbrecht, and U. Scherf, Adv. Funt. Mat. 16 (2006) 2156-2162.
7. A. M. Nardes, M. Kemerink, M. M. De Kok, E. Vinken, K. Maturova, and R. A. J. Janssen, Org. Electron. 9 (2008) 727-734.
8. F. So and D. Kondakov, Adv. Mater. 22 (2010) 3762-3777.
9. G. Li, C. W. Chu, V. Shrotriya, J. Huang, and Y. Yang, Appl. Phys. Lett. 88 (2006) 253503-1 -253503-3.
10. C. H. Hsieh, Y. J. Cheng, P. J. Li, C. H. Chen, M. Dubosc, R. M. Liang, and C. S. Hsu, J. Am. Chem. Soc. 132 (2010) 4887-4893.
11. A. K. K. Kyaw, X. W. Sun, C. Y. Jiang, G. Q. Lo, D. W. Zhao, and D. L. Kwong, Appl. Phys. Lett. 93 (2008) 221107-1-221107-3.
12. D. W. Zhao, S. T. Tan, L. Ke, P. Liu, A. K. K. Kyaw, X. W. Sun, G. Q. Lo, and D. L. Kwong, Sol. Energy. Mater. Sol. Cells 94 (2010) 985-991.
13. K. H. Tsai, J. S. Huang, M. Y. Liu, C. H. Chao, C. Y. Lee, S. C. Hung, and C. F. Lin, J. Electrochem. Soc. 156 (2009) B1188-B1191.
14. M. Lira-Cantu, K. Norrman, J. W. Andreasen, and F. C. Krebs, Chem. Mater. 18 (2006) 5684-5690.
15. H. Oh, J. Krantz, I. Litzov, T. Stubhan, L. Pinna, and C. J. Brabec, Sol. Energy. Mater. Sol. Cells. 95 (2011) 2194-2199.
16. M. L. Chantu, A. Chafiq, J. Faissat, I. G. Valls, and Y. Yu, Sol. Energy. Mater. Sol. Cells 95 (2011) 1362-1374.
17. H. F. Hussein, G. M. Shabeeb, and S. S. Hashim, J. Mater. Environ. Sci. 2 (2011) 423-426.
18. N. Duraisamy, N. M. Muhammad, M. T. Hyun, and K. Y. Choi, Mater. Lett. 92 (2013) 227-230.
19. M. Popa, R. A. Mereu, M. Filip, M. Gabor, M. Petrisor Jr, L. Ciontea, and T. Petrisor, Mater. Lett. 92 (2013) 267-270.
20. L. J. A. Koster, M. Kemerink, M. M. Wienk, K. Maturova, and R. A. J. Janssen, Adv. Mater. 23 (2011) 1670-1674.
21. S. Han, W. S. Shin, M. Seo, D. Gupta, S. J. Moon, and S. Yoo, Org. Electron. 10 (2009) 791-797.
22. Irfan, H. Ding, Y. Gao, C. Small, D. Y. Kim, J. Subbiah, and F. So, Appl. Phys. Lett. 96 (2010) 243307-1-243307-3.
23. J. Zou, H. L. Yip, S. K. Hau, and A. K. Y. Jen, Appl. Phys. Lett. 96 (2010) 203301-1-203301-3.
24. M. F. Xu, L. S. Cui, X. Z. Zhu, C. H. Gao, X. B. Shi, Z. M. Jin, Z. K. Wang, and L. S. Liao, Org. Electronics 14 (2013) 657-664.